

Stochastic Fuzzy Modeling for Ear Imaging Base Child Identification

Renuka D, Suganthi M^{*}, E.Valarmathi,K.Sivasakthi

*Nandha college of Engineering,
Erode, Tamilnadu, India.*

*Corresponding Author: D. Renuka

E-mail: renukaece127@gmail.com,

Received: 18/11/2015, Revised: 12/12/2015 and Accepted: 11/03/2016

Abstract

The unique identification of children is crucial for information technology supported vaccine delivery to the unprivileged population of third world countries. New robust image matching algorithms are required to match two ear photographs taken under nonstandard real-world conditions such as the presence of unwanted background objects in the photographs. This paper applies stochastic fuzzy models to the robust matching of ear images. The local features of the image regions are extracted using a “force-field-like” transformation. The extracted features of an image region are modeled by a stochastic fuzzy system. A region of an image is matched to a region of another image by matching the features of an image’s region with the model of another image’s region. As the model is fuzzy as well as stochastic, a robust matching of features’ data to a model is facilitated by handling any uncertainties arising from fuzziness and randomness of the image features. The study introduces an information-theoretic index for measuring the degree of matching between image features and a model of the features. Several experiments are performed on a database of 750 ear-photographs of children (0–6 years) to justify the novel stochastic fuzzy image matching method.

Keywords: Features, fuzzy models, image matching, robustness, Student-t distribution, variational Bayes.

**Reviewed by ICETSET'16 organizing committee*

1. Introduction

Immunization is the most cost effective medical intervention to reduce the mortality rates for infants and children under five. We are developing a concept of mobile phone based child identification for improved immunization in developing countries under a collaborative project between the “Center for Life Science Automation, Rostock, Germany,”

“Shah Satnamji Green-S Welfare Force Wing, Sirsa, India.” The child’s ear photograph taken by a mobile phone must be matched with in-database existing ear photographs for an accurate identification of small children and infants. This is of significance in information technology supported health care delivery to the underprivileged

population of developing countries where a reliable mechanism for the identification and registration of the masses is not in place. The problem of ear imaging based child identification is challenging due to the changes in the photographic conditions (such as illumination distance of camera, viewpoint, background, and so on) and the presence of unwanted objects in the background of the photograph. Therefore, a robust matching of photographs is required. Matching of similar structures between digital images is a fundamental step in computer vision and image processing applications. There is always an interest in comparing the objects' shape between two images. A shape descriptor that captures the distribution of the points relative to a reference point was proposed in [1]. Hausdorff distance is a widely used mathematical construct for measuring the distance between two edge maps (i.e., point datasets) and this distance can be calculated without requiring any correspondence between the points [2]. Mahalanobis distance is another metric applied for image processing applications [3]. The state-of-the-art algorithms typically identify the regions of interest in images, associate scale/rotation invariant descriptors to each region, and finally descriptors are matched to establish correspondences between the images' regions. This is referred to as local features based matching of images. The milestone work [4] introduced a scale-invariant feature transform (SIFT) that first uses difference-of-Gaussian region detector and then calculates descriptors based on the gradient orientation distribution in the region. The local features can be matched by defining a suitable dissimilarity measure between features and a matching criterion [5]. Also, the local features can be used with the machine learning methods for object classification [6]. The SIFT methods are the best known techniques for image matching applications as these methods are invariant to image scaling and rotation and partially invariant to illumination and viewpoint changes. The SIFT method has been extended to a fully affine invariant image matching framework [7]. It is natural that fuzzy researchers are motivated to exploit the uncertainty handling potential of fuzzy systems in robust image matching. Biswas *et al.* [8] have proposed the comparing of fuzzy membership-distance products, called moment descriptors, for image matching. Also, the fuzzy transform of an image can be compared with the fuzzy transform of another image to measure the grade of similarity between two images [9]. Kumar *et al.* [13]–[15] have recently introduced the stochastic fuzzy models that potentially may serve as a useful signal analysis tool in the presence of uncertainties. The main motivation of this paper is to validate the hypothesis that the mathematical theory of stochastic fuzzy models is capable of handling any of the image features. The salient features of the stochastic fuzzy approach to image matching are as follows. The image is processed by a transformation similar (but not identical) to the force field [16]. The transformation reinforces the edges and extracts the image features. A finite number of sub-images are created by the fuzzy *c*-means clustering of the position coordinates of stronger edges. A fuzzy clustering based Takagi–Sugeno fuzzy model is meant for the modeling of the image features. It is assumed that the image features are contaminated with the noises. The parameters of the stochastic fuzzy model are inferred under variational Bayes framework [17]–[21] and robustness is achieved by modeling the noises with the Student-t distributions [22], [23]. This paper introduces an information-theoretic index for measuring the degree of matching between image features and a model of the features. The matching score between data and a model is

defined as the average value of log-likelihood when parameters of the stochastic model are drawn from those variational distributions that maximize a lower bound on mutual information. Each subimage of an image is matched with all of the subimages of other image. The pair of sub-images with the highest matching scores corresponds to the “similar” regions in the two images. The literature on image processing algorithms is vast. However, uncertainty handling capabilities of fuzzy models have not been exploited till now to find out the similar regions in the two images under the wide range of photographic conditions. To the authors’ best knowledge, this is the first study to apply stochastic fuzzy models for robust matching of the objects appearing in different images. The methodology has been developed for the ear imaging based unique identification of infants and young children in information technology supported health care delivery to the unprivileged population of third world countries. The novelties and original contributions of this paper are as follows.

- 1) The idea of identifying infants and children via ear imaging for information technology supported vaccine delivery in developing countries is novel.
- 2) The modeling of the image features through a stochastic fuzzy system with Student-t distributed inputs/output noises and using an information-theoretic matching degree, instead of directly matching the image features, are the novelties of this paper.
- 3) The study introduces and derives analytically in Section IV the matching score between data and

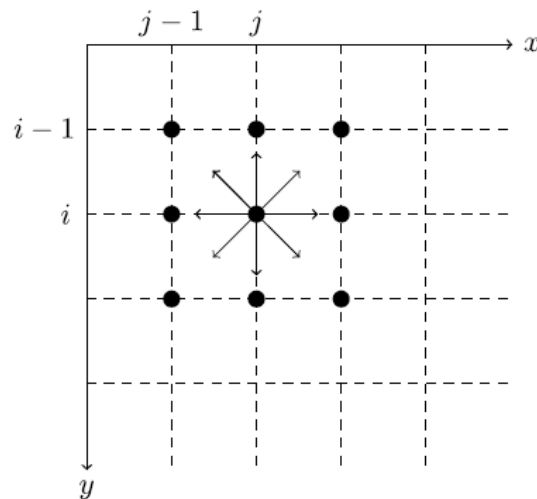


Fig. 1. Force experienced by a pixel due to the immediate neighboring pixels is calculated by using principle-of-superposition.

a model. The matching score is defined as the average value of log-likelihood when parameters of the stochastic model are drawn from those variational distributions that maximize a lower bound on mutual information.

- 4) A database of 750 ear photographs of children (0–6 years) built by taking photographs through a mobile phone under the field conditions of immunization has been studied in Section VI. The study validates the following argument: “while a direct matching of the image features is not sufficient to achieve robustness against real-world photographic conditions, the application of stochastic fuzzy theory together with an

informationtheoreticsimilarity measure is an effective approach forrobust matching of image regions. Thus, the proposedmethod was observed performing better than the benchmarkimage matching methods of histograms of orientedgradients (HOGs) [24], SIFT[4], speeded-up robustfeatures (SURFs) [25], and affine-SIFT (ASIFT) [7] in matching the ear-geometries between the two photographswhich have been taken under field conditions.”

2. Image Features Extraction

In the context of ear biometrics, Hurley *et al.* [16] haveintroduced a force field transformation where the image istreated as an array of Gaussian attractors that act as thesource of a force field. We introduce here similar to the studyof [16] another force-field-like transformation. With referenceto Fig. 1, it is assumed that each pixel of the image attractsall of its eight neighboring pixels toward itself with a forcesuch that the magnitude of force is directly proportional to theproduct of intensities of the two pixels and is inversely proportionalto the square of the distance

$$\vec{F}_{ij} = \sum_{i',j'} \frac{I(i,j)I(i',j')}{\|\vec{p}(i',j') - \vec{p}(i,j)\|^3} (\vec{p}(i',j') - \vec{p}(i,j))$$

between the two pixels.

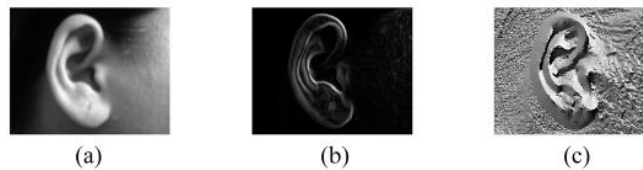


Fig. 2. Force-field like transformation of an ear image assuming a neighborhood of eight pixels. (a) Ear photograph. (b) Magnitude of force. (c) Direction of force.

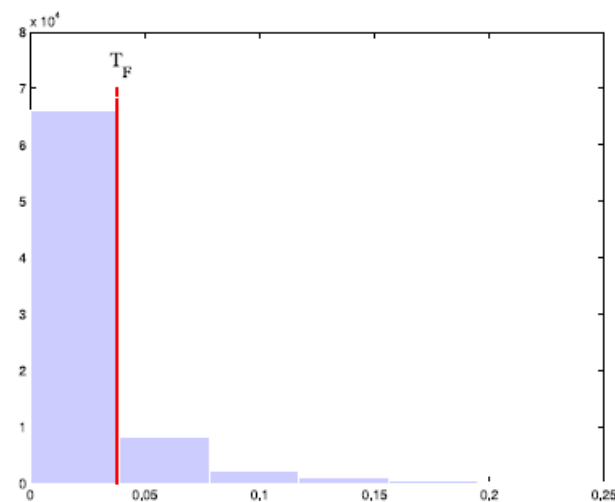
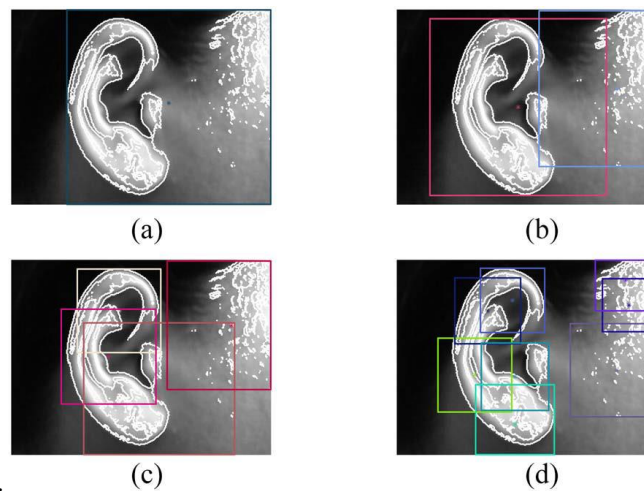


Fig. 3. Example of the histogram of force magnitude values for an image.

First, a pixel experiences forces only from its eight immediate neighboring pixels and not from all of the image pixels. Second, the transformation of [16], unlike here introduced transformation, assumes a unit intensity of the pixel at which force due to other pixels is calculated. As force is a vector quantity, it is possible to calculate magnitude and direction.

Remark 1: The choice of threshold value on force magnitude, proposed by (1), is derived from the experimental observations regarding the histogram of force magnitude values. Fig. 3 provides an example of the histogram of force magnitude values for an image. The threshold value, calculated by (1), is marked in Fig. 3. It can be observed from Fig. 3 that the proposed choice of threshold value clearly separates the edge-pixels from the pixels with a lower force magnitude. All the edge-pixels that are connected to at least one non edge pixel are referred to as boundary-pixels and have been marked in Fig. 4(a) as white dots. Once the boundary-pixels have been extracted, a square-sized block, bounding the boundary-pixels, can be drawn on the image. Fig. 4(a) also displays the boundary-block and its center. The position coordinates of boundary-pixels can be divided into a finite number of clusters using e.g., fuzzy *c*-means clustering. Further, a boundary-block could be drawn around the pixels of each cluster giving rise to a finite number of boundary-blocks. Fig. 4(b)–(d) displays the boundary-blocks for 2, 4, and 8 clusters, respectively. Please note that the overlapping between boundary-blocks exists as each boundary-block is forced to be of square-sized. The boundary-block is a subimage and one can extract within the block lying boundary-pixels by thresholding the force-magnitude as described previously, however, mean and variance are calculated locally



of the pixels lying within the block.

Fig. 4. Extraction of the boundary-pixels and their clustering. (a) Boundary pixels. (b) Number of clusters = 2. (c) Number of clusters = 4. (d) Number of clusters = 8.

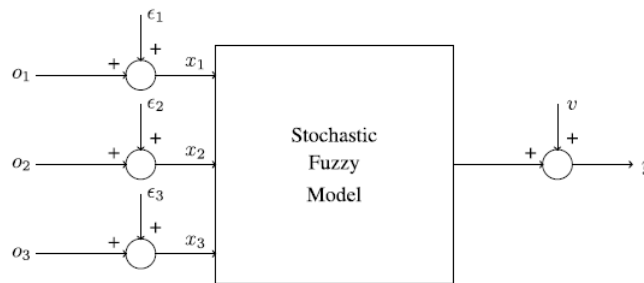


Fig. 5. Stochastic fuzzy modeling of image features.

3. Stochastic Fuzzy Modeling Of Image Features

It is assumed that the parameters (x_1, x_2, x_3, y) , defined by (2)–(5), are being affected by the additive disturbances $(\epsilon_1, \epsilon_2, \epsilon_3, v)$, respectively, and a stochastic fuzzy model identifies the relationship between input variables (x_1, x_2, x_3) and the output variable y . This modeling of image features is illustrated by Fig. 5. A fuzzy clustering based Takagi–Sugeno fuzzy model, described in Appendix A, was considered for the modeling of the image features. The model described in Fig. 5 is a three-inputs-single-output system. However, we formulate the modeling problem mathematically for a general n -inputs-single-output system.

Algorithm 1 Data Modeling Algorithm (as in [21])

Require: Inputs-output data pairs $\{x(k), y(k)\}_{k=1}^N$ and vectors $\{G(x(k))\}_{k=1}^N$ defined by the fuzzy model.

- 1: Choose initially the parameters of prior distributions as $\Lambda_o = I$, $\mu_o = 0$, $a_{x,\lambda} = b_{x,\lambda} = 10^{-3}$, $a_{x,d} = b_{x,d} = 10^{-3}$, $\Lambda_\alpha = I$, $a_{y,\lambda} = b_{y,\lambda} = 10^{-3}$, $a_{y,d} = b_{y,d} = 10^{-3}$.
 - 2: **while** ($k = 1, 2, \dots, N$) **do**
 - 3: Initialize the parameters of variational distributions as $\hat{\Lambda}_o = \Lambda_o$, $\hat{\mu}_o = \mu_o$, $\hat{a}_{x,\lambda} = a_{x,\lambda}$, $\hat{b}_{x,\lambda} = b_{x,\lambda}$, $\hat{a}_{x_j,z} = \hat{b}_{x_j,z} = 10^{-3}$, $\hat{a}_{x,d} = a_{x,d}$, $\hat{b}_{x,d} = b_{x,d}$, $\hat{\Lambda}_\alpha = \Lambda_\alpha$, $\hat{\mu}_\alpha = \mu_\alpha$, $\hat{a}_{y,\lambda} = a_{y,\lambda}$, $\hat{b}_{y,\lambda} = b_{y,\lambda}$, $\hat{a}_{y,z} = \hat{b}_{y,z} = 10^{-3}$, $\hat{a}_{y,d} = a_{y,d}$, $\hat{b}_{y,d} = b_{y,d}$.
 - 4: Update all the parameters of variational distributions with the data pair $(x(k), y(k))$ as per the equations listed in Result 1.
 - 5: The parameters updated with k -th data pair become prior for $(k + 1)$ -th data pair, i.e., $\Lambda_o = \hat{\Lambda}_o$, $\mu_o = \hat{\mu}_o$, $a_{x,\lambda} = \hat{a}_{x,\lambda}$, $b_{x,\lambda} = \hat{b}_{x,\lambda}$, $a_{x,d} = \hat{a}_{x,d}$, $b_{x,d} = \hat{b}_{x,d}$, $\Lambda_\alpha = \hat{\Lambda}_\alpha$, $\mu_\alpha = \hat{\mu}_\alpha$, $a_{y,\lambda} = \hat{a}_{y,\lambda}$, $b_{y,\lambda} = \hat{b}_{y,\lambda}$, $a_{y,d} = \hat{a}_{y,d}$, $b_{y,d} = \hat{b}_{y,d}$.
 - 6: $k \leftarrow k + 1$.
 - 7: **end while**
 - 8: **return** the parameters of variational distributions: $(\hat{\mu}_o, \hat{\Lambda}_o)$, $(\hat{a}_{x,\lambda}, \hat{b}_{x,\lambda})$, $(\hat{a}_{x,d}, \hat{b}_{x,d})$, $(\hat{\mu}_\alpha, \hat{\Lambda}_\alpha)$, $(\hat{a}_{y,\lambda}, \hat{b}_{y,\lambda})$, $(\hat{a}_{y,d}, \hat{b}_{y,d})$. The algorithm should also return the membership functions related parameters (i.e. cluster centers and variances) which are required to compute vector $G(\cdot)$.
-

Algorithm 2 Data Matching Algorithm

Require: Inputs-output data pairs $\{x(k), y(k)\}_{k=1}^N$ to be matched; the parameters of prior distributions: (μ_o, Λ_o) , $(a_{x,\lambda}, b_{x,\lambda})$, $(a_{x,d}, b_{x,d})$, $(\mu_\alpha, \Lambda_\alpha)$, $(a_{y,\lambda}, b_{y,\lambda})$, $(a_{y,d}, b_{y,d})$; and the membership functions related parameters required to compute vectors $\{G(x(k))\}_{k=1}^N$. Please note that the parameters of prior distributions and of membership functions completely characterize a model and have been returned (i.e., estimated) by running Algorithm 1 on some other dataset.

- 1: Initialize the parameters of variational distributions as $\hat{\Lambda}_o = \Lambda_o$, $\hat{\mu}_o = \mu_o$, $\hat{a}_{x,\lambda} = a_{x,\lambda}$, $\hat{b}_{x,\lambda} = b_{x,\lambda}$, $\hat{a}_{x_j,z} = \hat{b}_{x_j,z} = 10^{-3}$, $\hat{a}_{x,d} = a_{x,d}$, $\hat{b}_{x,d} = b_{x,d}$, $\hat{\Lambda}_\alpha = \Lambda_\alpha$, $\hat{\mu}_\alpha = \mu_\alpha$, $\hat{a}_{y,\lambda} = a_{y,\lambda}$, $\hat{b}_{y,\lambda} = b_{y,\lambda}$, $\hat{a}_{y,z} = \hat{b}_{y,z} = 10^{-3}$, $\hat{a}_{y,d} = a_{y,d}$, $\hat{b}_{y,d} = b_{y,d}$.
 - 2: Update all the parameters of variational distributions with the data pairs $\{x(k), y(k)\}_{k=1}^N$ as per the equations listed in Result 2 where expectations over $p(x, y)$ are calculated by using sample averages.
 - 3: Apply Result 3 on data pairs $\{x(k), y(k)\}_{k=1}^N$ with the updated parameters of variational distributions to calculate MS. Again, the expectations over $p(x, y)$ are calculated by using sample averages.
 - 4: **return** Matching score MS.
-

Taking expectation over $p(x, y)$, we have

$$\begin{aligned}
 & \left\langle \int \partial \Omega q^*(\Omega) \log(p(x, y|\Omega)) \right\rangle_{p(x,y)} \\
 &= -\frac{n+1}{2} \log(2\pi) + \frac{n}{2} \langle \log(\lambda_x) \rangle_{q^*(\lambda_x)} \\
 &+ \frac{1}{2} \sum_{j=1}^n \langle \log(z_{x_j}) \rangle_{q^*(z_{x_j})} - \frac{1}{2} \langle \lambda_x \rangle_{q^*(\lambda_x)} \\
 &\times \left\langle \left\langle (x-o)^T \begin{bmatrix} \langle z_{x_1} \rangle_{q^*(z_{x_1})} & & \\ & \dots & \\ & & \langle z_{x_n} \rangle_{q^*(z_{x_n})} \end{bmatrix} (x-o) \right\rangle_{q^*(o)} \right\rangle_{p(x)} \\
 &+ \frac{1}{2} \langle \log(\lambda_y) \rangle_{q^*(\lambda_y)} + \frac{1}{2} \langle \log(z_y) \rangle_{q^*(z_y)} \\
 &- \frac{1}{2} \langle \lambda_y \rangle_{q^*(\lambda_y)} \langle z_y \rangle_{q^*(z_y)} \left\langle \left\langle |y - (G(x))^T \alpha|^2 \right\rangle_{q^*(\alpha)} \right\rangle_{p(x,y)}.
 \end{aligned}$$

4. Image Matching Algorithm

Finally, all of the theoretical results presented in this paper are carefully put together to develop an image matching algorithm (Algorithm 3) for finding the similar regions in two images and giving an overall matching degree between the two images. The functionality of Algorithm 3 is as follows.

- 1) First of all, K sub-images of image I_a and K sub-images of image I_b are created.
- 2) The image features associated to each boundary-block are modeled by Algorithm 1 provided that the boundary block has at least 500 data points. The reason for setting the requirement of 500 data points is that the inferred stochastic fuzzy model might not be sufficiently accurate if the number of data points is not sufficiently large. An inaccurate model leads to dubious matching results.
- 3) Each subimage (referred to as boundary-block) of an image is matched with all of the sub-images of other image at steps 11 and 12.
- 4) The i th subimage of image I_a is considered matched to the j th subimage of image I_b , if:
 - a) i th subimage of image I_a matches highest to j th subimage of image I_b ;
 - b) j th subimage of image I_b matches highest to i th

subimage of image I_a .

5) The pairs of matching sub-images correspond to the similar regions in the two images.

6) Each pair of matching sub-images contributes to the overall matching degree between the images at step 18. The algorithms were implemented using MATLAB R2014a. The computational time required by Algorithm 3 depends upon the number of boundary-blocks processed by the algorithm and the number of boundary-pixels associated to each boundary-block. Algorithm 3 hardly makes computations but invokes multiple times the Algorithm 1 for modeling and Algorithm 2 for matching. It was observed that for a subimage with N boundary-pixels, a nonoptimized MATLAB code on a MacBook Pro machine with a 2.9-GHz Intel Core i7 processor results in the modeling time in milli-seconds $\approx 1.95 \times N$ the matching time in milli-seconds $\approx 0.45 \times N$.

5. Ear Imaging For Child Identification

The considered application example is concerned with the unique identification of infants and young children for information technology supported vaccine delivery to the unprivileged population of third world countries. We have proposed a mobile phone based identification and vaccination information management system that addresses the global health problem of no or incomplete vaccination of children by effectively reaching the children through community workers, identifying the mother-child unit, educating the people about immunization programs, and electronically documenting the immunization events. The integrated camera of the mobile phone is used to take the child's ear photograph. A mobile application facilitates the comparison of child's ear photograph within the server's database existing candidate photographs to find the most matching ear photograph. The identity of the child is verified by the community health worker depending upon if the personal details of the child of query photograph match with the personal details of the child of most matching photograph. Our approach is to use the benchmark SIFT method to quickly scan the database for generating the candidate photographs. Algorithm 3 can be run on relatively small number of candidate photographs for robust matching. The application, due to a relatively small number of candidate photographs, does not pose a challenge in terms of the computation time of the image matching algorithm but in terms of the robustness. A robust image matching algorithm, capable of performing identification under real-world photographic conditions (such as the presence of unwanted background objects in the photographs), is demanded. Furthermore, the algorithm is desired to be robust toward factors such as illumination, distance of camera, and viewpoint. To demonstrate the effectiveness of the Algorithm 3 in robust matching of ear images, a database of 750 ear photographs of children (0–6 years) is studied. The database might include up to five different ear photographs of the same child which have been taken at different points of time under different photographic conditions. Fig. 6 displays a few samples from the database which act as the query photographs to demonstrate the application potential of the proposed method. The ground truth of each query photograph is another photograph of the ear of the same child in the database. For a given query photograph, the candidate photographs are generated by a quick scan of database by SIFT method as follows.

1) All the photographs of database are ranked as per their number of SIFT key-point matches.

2) The photographs, achieving a rank (as per the SIFT method) higher than or equal to the rank of a child's ear photograph with the same name and date-of-birth as the name and date-of-birth of the child of query photograph, serve as the candidate photographs for Algorithm 3 and other considered image matching methods.

Remark 3: As ear images are differently scaled, a simple correlation between the images cannot be used to generate the candidate photographs. Therefore, SIFT, being scale invariant, was used to generate the candidate photographs. It is observed for SIFT that despite some wrong key-point matches, the number of matching key-points between two images increases considerably in the case of a common object between two photographs. Thus, photographs have been ranked as per number of SIFT key-point matches. Fig. 7 displays the most matching photographs to the query photographs found by SIFT. As observed from Fig. 7, the key-points lying on background regions affect adversely and thus lead to the incorrect matching of ear photographs. Therefore, a method robust to real-world photographic conditions is required. To directly match the image features without applying stochastic fuzzy theory, the following methodologies are considered.

- 1) HOGs features [24] encode local shape information from regions within an image and thus the inverse squared Euclidean distance between the HOG features of two images is a measure of the similarity between two images.
- 2) The number of key-point matches between two images found by widely used SIFT method is a measure of the similarity between two images.
- 3) Similarly to SIFT, the SURFs [25] is another image matching method defining the descriptor based on the spatial distribution of first-order Haar wavelet responses in the x - and y -direction. The SURF could be more robust against different image transformations than SIFT. The number of key-point matches between two images found by SURF method is a measure of the similarity between two images.
- 4) ASIFT [7] is a fully affine invariant image comparison method that allows to reliably identify image features under very large affine distortions. The number of key-point matches between two images found by ASIFT method is a measure of the similarity between two images.

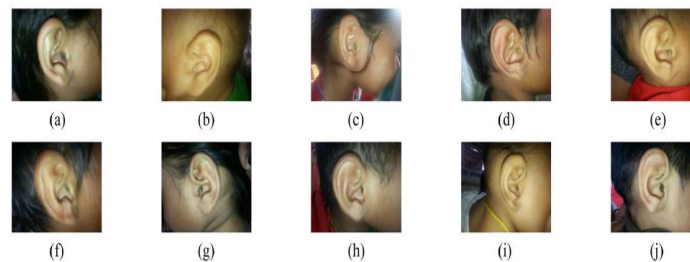


Fig. 6. Few samples from the database of children’s ear photographs. (a) Query photograph 1. (b) Query photograph 2. (c) Query photograph 3. (d) Query photograph 4. (e) Query photograph 5. (f) Query photograph 6. (g) Query photograph 7. (h) Query photograph 8. (i) Query photograph 9. (j) Query photograph 10.

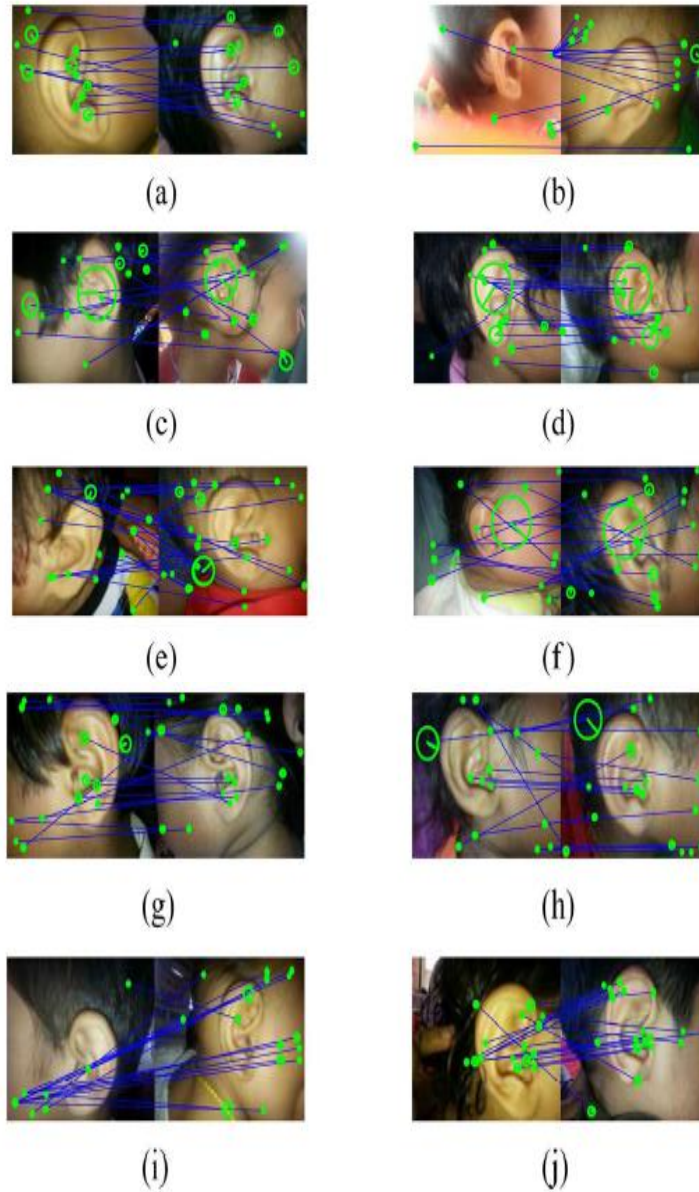


Fig. 7. Most matching photographs to the query photographs found by SIFT. (a) Query photograph 1. (b) Query photograph 2. (c) Query photograph 3. (d) Query photograph 4. (e) Query photograph 5. (f) Query photograph 6. (g) Query photograph 7. (h) Query photograph 8. (i) Query photograph 9. (j) Query photograph 10.

TABLE I
COMPARISON OF DIFFERENT METHODS IN TERMS OF
NUMBER OF CORRECTLY IDENTIFIED CHILDREN

method	correct identifications by most matching photo
Algorithm 3	10
HOG	5
SIFT	0
SURF	4
ASIFT	4

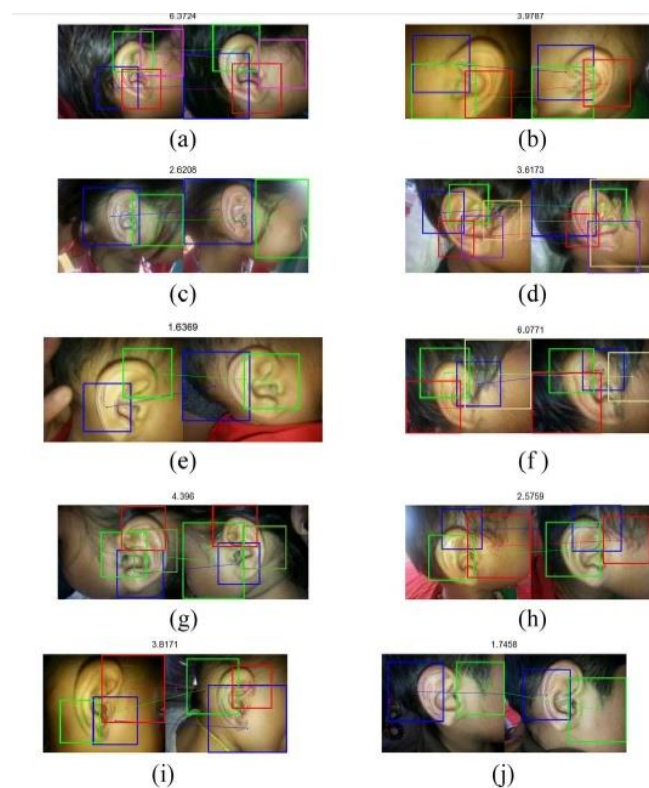


Fig. 8. Most matching photographs to the query photographs found by Algorithm 3. (a) Query photograph 1. (b) Query photograph 2. (c) Query photograph 3. (d) Query photograph 4. (e) Query photograph 5. (f) Query photograph 6. (g) Query photograph 7. (h) Query photograph 8. (i) Query photograph 9. (j) Query photograph 10.

The different methods were compared in terms of the number of correctly identified children. Table I lists the number of times a method could find the true match in ten different examples of query photographs, i.e., the number of times the best matching photograph to a query photograph is same as the ground truth of the query

photograph. As observed from Table I, none of the considered methods (i.e., HOG, SIFT, SURF, and ASIFT), unlike the proposed method, could correctly identify the ear photograph in all of the ten examples. The found matches by Algorithm 3 have been displayed in Fig. 8. To objectify the performance of different methods, a pool of candidate photographs is created by accumulating the candidate photographs of all the ten query photographs. The so created pool contained in total 152 ear photographs. For each of the query photographs, a binary classifier was built to classify any candidate photograph from the pool either as true match or false match. The classifier, for a given image matching method, thresholds the matching score between query and candidate photograph to classify the candidate photograph. The classification performance of different methods is compared by studying their receiver operating characteristic (ROC) curves. Fig. 9 plots the ROC curve and Table II reports the area under ROC curve for the considered methods. The better performance of Algorithm 3 than HOG, SIFT, SURF, and ASIFT methods is clearly observed from Fig. 9 and Table II.

The experimental results validate the argument that while a direct matching of the image features (calculated by HOG, SIFT, SURF, and ASIFT methods) is not sufficient to achieve robustness against real-world photographic conditions, the application of stochastic fuzzy theory together with an information-theoretic similarity measure is an effective approach for robust matching of image regions. Thus, the stochastic fuzzy theory offers a promising method for ear imaging based identification of infants and young children under real world photographic conditions.

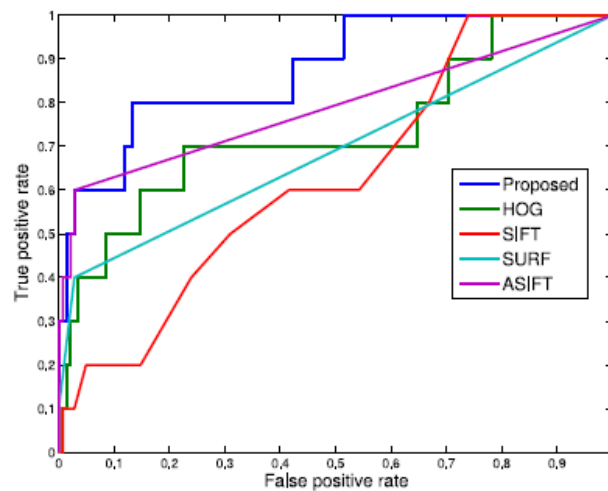


Fig. 9. ROC curves for proposed, HOG, SIFT, SURF, and ASIFT methods.

TABLE II
COMPARISON OF DIFFERENT METHODS IN TERMS
OF CLASSIFICATION PERFORMANCE

method	area under ROC curve
Algorithm 3	0.875352
HOG	0.733099
SIFT	0.630986
SURF	0.687324
ASIFT	0.788732

6. Conclusion

This paper has formulated the image matching problem in the framework of fuzzy modeling. The most important contribution of this paper is to apply the mathematical theory of stochastic fuzzy models to define a robust matching score between two images. The theoretical results are independent of the choice of image features and thus the proposed approach can be used with any choice of the image features. The currently used image features are in their most basic forms and thus several modifications can be tried. Despite a very simple choice of image features the robustness of the image matching algorithm is attributed to the effectiveness of stochastic fuzzy theory in dealing with the uncertainties. Algorithm 3, a robust image matching algorithm, was observed to be effective for a robust matching of ear-geometries between the two photographs which have been taken without controlled conditions. It is our future research task to extend the proposed method to a technique with applications to computer vision.

REFERENCES

- [1] S. Belongie, J. Malik, and J. Puzicha, "Shape matching and object recognition using shape contexts," *IEEE Trans. Pattern Anal. Mach. Intell.*, vol. 24, no. 4, pp. 509–522, Apr. 2002.
- [2] C.-H. T. Yang, S.-H. Lai, and L.-W. Chang, "Hybrid image matching combining Hausdorff distance with normalized gradient matching," *Pattern Recognit.*, vol. 40, no. 4, pp. 1173–1181, 2007.
- [3] S. Xiang, F. Nie, and C. Zhang, "Learning a Mahalanobis distance metric for data clustering and classification," *Pattern Recognit.*, vol. 41, no. 12, pp. 3600–3612, Dec. 2008.
- [4] D. G. Lowe, "Distinctive image features from scale-invariant keypoints," *Int. J. Comput. Vis.*, vol. 60, no. 2, pp. 91–110, Nov. 2004.
- [5] J. Rabin, J. Delon, and Y. Gousseau, "A statistical approach to the matching of local features," *SIAM J. Imag. Sci.*, vol. 2, no. 3, pp. 931–958, 2009.
- [6] T. Deselaers, G. Heigold, and H. Ney, "Object classification by fusing SVMs and Gaussian mixtures," *Pattern Recognit.*, vol. 43, no. 7, pp. 2476–2484, 2010.
- [7] J.-M. Morel and G. Yu, "ASIFT: A new framework for fully affine invariant image comparison," *SIAM J. Imag. Sci.*, vol. 2, no. 2, pp. 438–469, 2009.
- [8] B. Biswas, A. Konar, and A. K. Mukherjee, "Image matching with fuzzy moment descriptors," *Eng. Appl. Artif. Intell.*, vol. 14, no. 1, pp. 43–49, 2001.
- [9] F. D. Martino and S. Sessa, "Image matching by using fuzzy transforms," *Adv. Fuzzy Syst.*, vol. 2013, Jan. 2013, Art. ID 760704.
- [10] M. Amiri and H. R. Rabiee, "A novel rotation/scale invariant template matching algorithm using weighted adaptive lifting scheme transform,"